Original Article

Possible Ameliorating Role of Grape Seed Proanthocyanidin Extract on Seminiferous Tubules Toxicity Induced by Aluminium Oxide Nanoparticles in Adult Rats: Histological and Biochemical Study

Iman Nabil[1], Marwa Mahmoud Mady[2] and Silvia Kamil Seddik Sawires[1]

[1]Department of Histology and Cell Biology, [2]Department of Anatomy and Embryology, Faculty of Medicine, University of Alexandria

ABSTRACT

Introduction: Although aluminum oxide nanoparticles (Al2O3-NPs) are widely used, their possible hazards on male reproduction are not fully studied. Overproduction of oxidant species is the main mechanism of Al2O3-NPs induced histological changes in many organs. Grape seed proanthocyanidin extract (GSPE) is a powerful antioxidant compound, which might alleviate these effects.

Aim of the Work: To assess the histological and biochemical changes induced by Al2O3-NPs on adult rat seminiferous tubules and the probable role of proanthocyanidin in attenuating these changes.

Materials and Methods: 24 adult male albino rats were divided into 4 equal groups: group I (Control group), group II received oral GSPE at a dose of 100 mg/kg/day, group III received 70 mg/kg/day of Al2O3-NPs orally, and group IV co-administrated GSPE and Al2O3-NPs at the same doses as in groups II and III. The rats were sacrificed after 28 days, blood samples were obtained for biochemical analysis. Semen samples were taken to measure sperm count and motile sperm percent. The testes were weighed and then processed for light and electron microscopic examination and calculation of Johnsen score. Statistical analyses of the obtained data were performed.

Results: Al2O3-NPs induced vacuolations and decline in the number of the lining cells of the seminiferous tubules. Degenerated and exfoliated spermatogenic cells were found together with abnormal sperm heads and tails. Additionally, disrupted blood testis barrier and Sertoli cells degenerative changes were seen. A statistically significant reduction in the levels of serum testosterone, antioxidant markers, Johnsen score, sperm parameters together with a statistically significant elevation in the oxidant profiles were noticed. Concomitant administration of GSPE with Al2O3-NPs resulted in improvement in the structure of the testis with restoration of nearly normal level of testosterone, antioxidant capacity and semen analysis.

Conclusion: GSPE ameliorates the testicular histochemical changes induced by the Al2O3-NPs. Public awareness of GSPE importance is essential.

Received: 15 May 2022, **Accepted:** 17 July 2022

Key Words: Aluminium oxide nanoparticles, grape seed extracts, oxidative stress, testis.

Corresponding Author: Silvia Kamil Seddik Sawires, PhD, Department of Histology and Cell Biology, Faculty of Medicine, University of Alexandria, Egypt, **Tel.**: +20 12 2695 0510, **E-mail:** silviakamil76@yahoo.com

ISSN: 1110-0559, Vol. 46, No. 3

INTRODUCTION

Nanotechnology is now a rapidly-developing science which deals with and manages particles measured in nanoscale[1]. It is a multidisciplinary field engaging many other specialties including cell biology, molecular biology, physics, medicine and engineering[2]. Owing to the small size of the nanoparticles (NPs), their application is booming in different medical and industrial fields[3].

Recently, huge advances are achieved in the preparation of the NPs in order to improve their properties[4,5] such as bioavailability[6], biocompatibility[7], agglomeration[8]and dispersion[9]. The main concern is to provide novel and more safety applications of these particles in many fields including biomedicine[10,11]. Several uses of NPs are applied in medicine especially in the delivery of chemotherapeutic agents, antibiotics, antiviral drugs[4,5] and even vaccines[6]. Additionally, they are being used in polymer coating[7], diagnostic imaging[8], phototherapy in cancer treatment[9] and as a catalyst in many reactions[10].

Aluminum Oxide Nanoparticles (Al2O3-NPs) are considered nowadays one of the metal oxide nanoparticles (MONPs) that are most commonly used worldwide. Due to their distinct physiochemical properties, they are considered to be superb NPs in manufactures[12,13]. Commercially, they stand among the two market leaders of nanomaterials in USA[14]. They are extensively utilized in industries as carriers to improve the drug solubility[15], in adjustment of polymers, ceramics industries, fabrication of textiles[16], aerospace, electronics like production of electrical pieces and batteries[17], in cosmetics and water treatment[18].

The inevitable exposure to Al2O3-NPs has been greatly raised which creates a hot debate about their impact on the human health. Recently, it has been found that MONPs

Personal non-commercial use only. EJH copyright © 2023. All rights served *DOI: 10.21608/ejh.2022.138527.1684*

can permeate biological barriers like the blood–brain barrier and blood–testis barrier causing diverse adverse effects[19,20]. Moreover, many researchers studied the effect of AL2O3-NPs exposure during pregnancy and stated that neurotoxicity was found in the offsprings of the exposed pregnant mice. In this context, the particles were detected in many organs such as kidney, liver and brain, ultimately leading to genotoxicity both in *vivo* and in *vitro*[21,22].

Over the past few decades, human infertility in male was considered a progressively increasing problem[23], which incriminates the environmental exposure to toxic pollution[24]. Additionally, the testis is one of the organs that are more prone to environmental hazards including chemical toxins, pollution or even NPs[25,26].

Among the underlying mechanisms of AL2O3-NPs toxicity is the increasing level of reactive oxygen species, release of inflammatory mediators and eventually cell death. The main cellular targets of alumina are the nucleus and mitochondria. Broadly speaking, these NPs can induce mutation in DNA as well as sever mitochondrial damage[27].

Owing to The unhealthy life style of the population in the last years especially in the developing countries, many health problems started to get more attention by the scientists. Public health education of the risk factors and causes of the diseases is essential in forestalling them. People are now interested in the search for a healthy diet in order to improve their physical and mental health status[28].

The grape vine is a vital plant globally used because of its beneficial effects on health. Several biologically active compounds are nominated within the plant seeds[29]. Proanthocyanidins (PACs) are considered the main natural product of grape seed extract, consisting of polyphenolic bioflavonoids[28,29].

It is well known that grape seed proanthcyanidin extract (GSPE) has a positive impact on human health due to its antioxidant, antiapoptotic and anti-inflammatory effects. These properties were emphasized while studying its role in the course of many chronic diseases as cancer, diabetes mellitus, obesity and cardiovascular diseases[30,31]. Moreover, GSPE possesses antiviral, antibacterial effects[32,33] as well as a potential preventive effect on human colon dysfunction[31].

The protective effect of GSPE is elicited by its ability to regulate the level of cell oxidative stress, to maintain the balance between oxidants and antioxidants, and to minimize the secretion of inflammatory cytokines[34,35].

To the best of our knowledge, no previous researches were done to study the toxicity of AL2O3-NPs on rats' testes at the ultrastructure level. Thus, the current research was conducted to study the potential toxic effect of AL2O3-NPs on rat seminiferous tubules, histologically (at the light and ultrastructural levels) and biochemically, and to investigate the possible alleviation of the structural and the biochemical changes by the natural grape seed proanthocyanidin extract.

MATERIALS AND METHODS

Chemicals

Al2O3-NPs (≤ 50 nm) white, solid nanopowder was obtained from Nanotech Company, Egypt.

Grape seed proanthocyanidin extract: was purchased, as a powder, from Sigma Chemical Company (St. Louis, MO, USA).

Characterization of Al2O3-NPs

Transmission electron microscopy (TEM)

TEM [(Jeol 1400 plus, Tokyo, Japan) at the Faculty of Science, University of Alexandria] was used for visualization of the NPs and measuring their sizes. A small drop of Al2O3-NPs was placed onto TEM grids, covered with carbon film and was left few hours in order to dry before examining the NPs morphology and measuring their sizes. Digital micrographs of different localities on the grid were obtained[36].

Zeta potential measurement

Sample of Al2O3-NPs was diluted in distilled water. The zeta potential was analyzed using a Nano Zetasizer particle analyzer (nanoseries, Malvern, UK) using the manufacturer provided software[14,37].

Animal grouping and experimental design

Animal treatment

The study was conducted at the animal house of Physiology Department, Alexandria Faculty of Medicine. Twenty four adult male albino rats weighing 150-200 g were used in this experiment. The animals were kept under standard conditions, with free access to water and standard rat food and in a controlled temperature, humidity and 12 hours light/dark cycle. All procedures were approved by the Alexandria University Faculty of Medicine's Local Medical Ethics Committee, IRB number 00012098, and conform to the criteria of animal care in the "Guide for the Care and Use of Laboratory Animals".

Acclimatization of the animals to the new environment was done, a week before the experiment. Rats were divided into 4 equal groups each included six rats as follows:

Group I (control group): received 1mg/kg normal saline.

Group II (GSPE group): received GSPE (100 mg/kg/d) dissolved in normal saline. In order to obtain a solution concentration of 10 mg/ml, an amount of 100 mg GSPE was dissolved in 10 mL normal saline. The oral dose of GSPE was determined based on the minimal effective dose in similar studies in animals[38] and on the recommended dose for GSE supplementation in humans[39].

Group III (Al2O3-NPs group): received 70 mg/kg/d Al2O3-NPs suspended in 1 ml distilled water (aqueous suspension)[40].

To avoid agglomeration and obtain an efficient size distribution, the suspending solution was ultrasonicated before its oral administration to rats[37].

Group IV (Al2O3-NPs+GSPE group): the animals were co-administrated GSPE and Al2O3-NPs aqueous suspensions at the same doses as in groups 2 and 3.

In all four groups, oral gavage was used to provide treatment on a daily basis for 28 days.

Sampling

Twenty-four hours after the end of the 28 days, all the rats received 1.9% inhaled diethyl ether (0.08 ml/liter of the container volume)[41]. For biochemical studies, blood samples were taken from the retro-orbital venous plexus of all rats and were left to clot. Centrifugation of the samples at 1000 xg for 15 minutes was done, sera were separated and stored at -20 oC. Rats were sacrificed, the epididymides were removed and processed for sperm count and motile sperm percent. The right and left testes were excised; their weights were recorded and then processed for histological study (light and electron microscopic examination respectively).

Biochemical analysis

Measuring of Serum Testosterone

Sera and reagents were brought down at room temperature on the time of the assay. Enzyme-linked immunosorbent assay (ELISA) kit (Abbott, Vienna, Austria.) was used for the quantitative measurement of plasma testosterone[42]. Measured testosterone was expressed in ng/mL.

The oxidant markers

Serum malondialdehyde (MDA)

One of the product of lipid peroxidation; MDA was measured in serum as an oxidative stress marker, using the MDA colorimetric assay by a Humalyzer junior photometer (Human diagnostics, Wiesbaden, Germany). MDA in the samples reacts with thiobarbituric acid (TBA) giving pink thiobarbituric acid reactive products (TBARPs) that can easily be quantified colorimetrically with a maximum absorbance at 532 nm[43].

Serum lactate dehydrogenase (LDH)

LDH is an oxidoreductase that increases in serum during oxidative stress[44]. Total LDH activity was determined using LDH (EC 1.1.1.27) colorimetric assay (abcam, MA, USA) following the manufacturer's instructions. Absorbance was measured at 450 nm.

The antioxidant markers

Serum superoxide dismutase (SOD)

SOD is an antioxidant enzyme that inhibits the reduction of nitro blue tetrazolium (nitroBT) in the presence of riboflavin. The absorbance of color is spectrophotometrically measured at 560 nm[45]. The activity of SOD was determined as U/ml.

Serum total antioxidant capacity (TAC)

TAC was determined using a colourimetric method by commercially available kit (Biodiagnostic Company, Egypt)[46]. Results were expressed as mM/L.

Sperm count and motile sperm percent

The epididymides of each rat were obtained, minced thoroughly in 1 mL phosphate buffered saline (PBS) at pH 7.2 and filtered through a mesh. 0.05 mL from the filtrate was diluted with PBS 1:40 and introduced to the Neubauer counting chamber. The number of sperm and motile sperm in eight squares (1mm2 each) was counted and multiplied by 5x104 to determine the total sperm count and percent of motile sperm per epididymis[47].

Histological study

Light microscopic study and Johnsen score

The right testis was fixed in Bouin's solution for 24 hours, followed by fixation in 10% formol saline and prepared to obtain 5 µm thick paraffin sections to be stained with hematoxylin and eosin stains[48]. By using Johnsen score for rats, the seminiferous tubules were evaluated. All tubules in one section were examined and given a score from one to 10 according to the degree of germ cell maturity (a score of 10 indicates maximum spermatogenesis activity, whereas a score of 1 indicates complete absence of germ cells). Then, the mean score was calculated by dividing the sum of scores by the number of the tubules examined[49].

Electron microscopic study

Each rat's left testis was promptly sliced into small pieces (about 1x1 mm3) and fixed in 3% gluteraldehyde buffered with 0.1 M phosphate buffer at pH 7.4. They were then post fixed in 1% osmium tetra oxide in the same buffer. Processing of the specimens was done and ultrathin sections were obtained and stained with uranyl acetate and lead citrate[50] and examined with TEM (Jeol 1400 plus, Tokyo, Japan) at the Faculty of Science, University of Alexandria.

Statistical analysis

Data (including serum testosterone, oxidants and antioxidant markers, semen parameters, testicular weight and Johnsen score) were calculated using a statistical software application and expressed as a mean + SD. Statistical analysis was conducted using ANOVA and the post-hoc test for pair wise comparison. *P value* ≤ 0.05 was considered a value of significance.

RESULTS

Characterization of the Al2O3-NPs

TEM examination of Al2O3-NPs showed that their sizes ranged from 7.31-12.43 nm (Figure 1). The zeta potential of Al2O3-NPs was -44.75 mV.

Testicular weight

On measuring the weight of the testes at the end of the experiment, no statistically significant difference was detected in the all experimental groups (Figure 2A).

Biochemical study

Serum testosterone

No statistically significant difference in the hormonal assay was found in groups I, II & IV. On the other hand, a statistically significant reduction in the level of serum testosterone was found in group III that received AL2O3-NPs in comparison with the other experimental groups ($p \leq 0.001$) (Figure 2B).

The oxidant markers

By measuring the serum levels of MDA and LDH, statistically significant higher levels of these markers were detected in group III in comparison to the other three experimental groups ($p \leq 0.001$) which showed no statistical difference among them (Figures 3 A,B).

The antioxidant markers

The serum levels of SOD showed statistically significant higher levels in groups I, II and IV in comparison with group III ($p \leq 0.001$) that depicted statistically significant lower levels of this marker. In comparing groups I, II, and IV, no statistically significant differences were observed among them (Figure 3C).

Meanwhile, the serum level of TAC revealed statistically insignificant difference in groups I and II. A statistically significant lower level of serum TAC was detected in group III which received AL2O3-NPs in comparison to groups I and II. Administration of GSPE with AL2O3-NPs in group IV resulted in an increase in the serum level of this marker but this elevation was statistically insignificant in comparison with the other experimental groups (Figure 3D).

Sperm count and motile sperm percent

In comparing groups I, II and IV, a normal sperm count was detected with no statistically significant difference among them. AL2O3-NPs group (group III) showed a statistically significant reduction in the sperm count in comparison with all other groups ($p \leq 0.001$) (Figure 4A).

There was no statistically significant difference in the percentage of motile sperm between groups I and II. On the other hand, a statistically significant increase in the motile sperm percent was observed in group IV in comparison to group III ($p \leq 0.001$), although this increase was significantly lower than groups I and II ($p \leq 0.001$). Group III depicted a statistically significant lower motile sperm percent than all other experimental groups ($p \leq 0.001$) (Figure 4B).

Histological changes

Johnsen score

A statistically significant lower Johnsen score was detected in group III compared to all other groups ($p \leq 0.001$) that showed no statistically significant differences between them (Figure 4C).

LM examination

Group I (Control group): Light microscopic examination of the control group showed multiple seminiferous tubules separated by a narrow interstitium. Each tubule was lined by Sertoli cells as well as spermatogenic cells. Sertoli cells could be distinguished by their large and pale nuclei. The most basal spermatogenic cells; spermatogonia, displayed rounded or oval nuclei. Primary spermatocytes showed large nuclei with their characteristic chromatin condensation. Early spermatids were the most apical cells with rounded nuclei. Numerous spermatozoa were filling the tubular lumen. Myoid cells with flat nuclei were seen surrounding the basal lamina (Figure 5A).

Group II (GSPE group): The seminiferous tubules of this group revealed normal structure regarding Sertoli and spermatogenic cells (Figure 5B).

Group III (AL2O3-NPs group): The histologic alterations in the seminiferous tubules and their lining cells in this group were quite obvious. Distortion of the normal architecture and irregularity of the tubules together with reduction in the number of the lining cells were noticed. Degenerating and exfoliated spermatogenic cells were encountered. Cellular changes in the form of cytoplasmic vacuolations as well as dark and small nuclei were observed. (Figures 6A-D).

Group IV (AL2O3-NPs + GSPE): Examination of this group showed apparently normal Sertoli cells as well as spermatogenic cells, although some histological changes appeared in few spermatogenic cells in the form of mild vacuolations and pyknotic nuclei (Figures 7 A,B).

EM examination

Group I (Control group): Ultrastructural examination of the seminiferous tubules showed a Sertoli cell with a large euchromatic nucleus with prominent nucleolus and multiple mitochondria. Two types of spermatogonia were depicted: type A spermatogonia with its ovoid nucleus and granular chromatin, and type B spermatogonia with their rounded nuclei and a peripheral condensed chromatin. An intact blood testis barrier (BTB) was observed above the level of the spermatogonia. The primary spermatocytes were noticed with their rounded nuclei and mitochondria. The early spermatids were recognized by their rounded euchromatic nuclei covered by the acrosomal cap and peripherally situated mitochondria. The sperm tail with its characteristic pieces were encountered in the lumen of the seminiferous tubules (Figures 8A-F).

Group II (GSPE group): Examination of the rat seminiferous tubules of this group revealed normal Sertoli cells as well as spermatogenic cells (Figures 9A-D).

Group III (AL2O3-NPs group): The seminiferous tubules of this group depicted significant ultrastructural changes affecting Sertoli and spermatogenic cells. Sertoli cells showed shrunken nucleus with chromatin disintegration, multiple vacuolations and rarified cytoplasm together with disrupted BTB. The spermatogenic cells revealed cytoplasmic and nuclear changes. Multiple cytoplasmic vacuolations were noticed. Nuclear changes in the form of degenerating nuclei, dilated perinuclear cisternae and ruptured nuclear envelope were all encountered. Abnormal heads and tails of the late spermatids were found. Middle pieces of the sperm tail with distorted dense fibers and mitochondrial sheath, principal pieces with interrupted circumferential ribs and end pieces with vacuolations were observed (Figures 10A-H).

Group IV (AL2O3-NPs + GSPE group): The rat testis of this group revealed apparently normal seminiferous tubules with their lining cells. Some foci of structural changes were depicted such as mild cytoplasmic vacuolations in Sertoli cells and spermatogonia (Figures 11A-F).

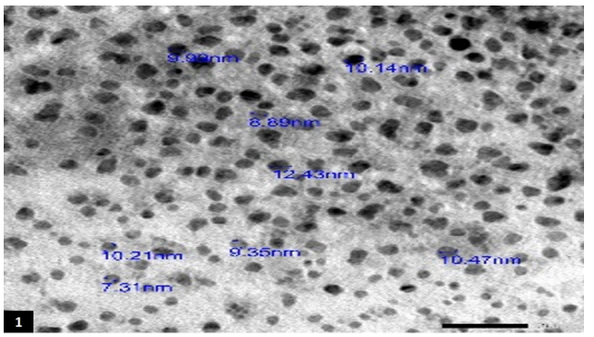

Fig. 1: TEM micrograph shows AL2O3-NPs with diameter size 7.31-12.43 nm. Mic. Mag.x100.000.

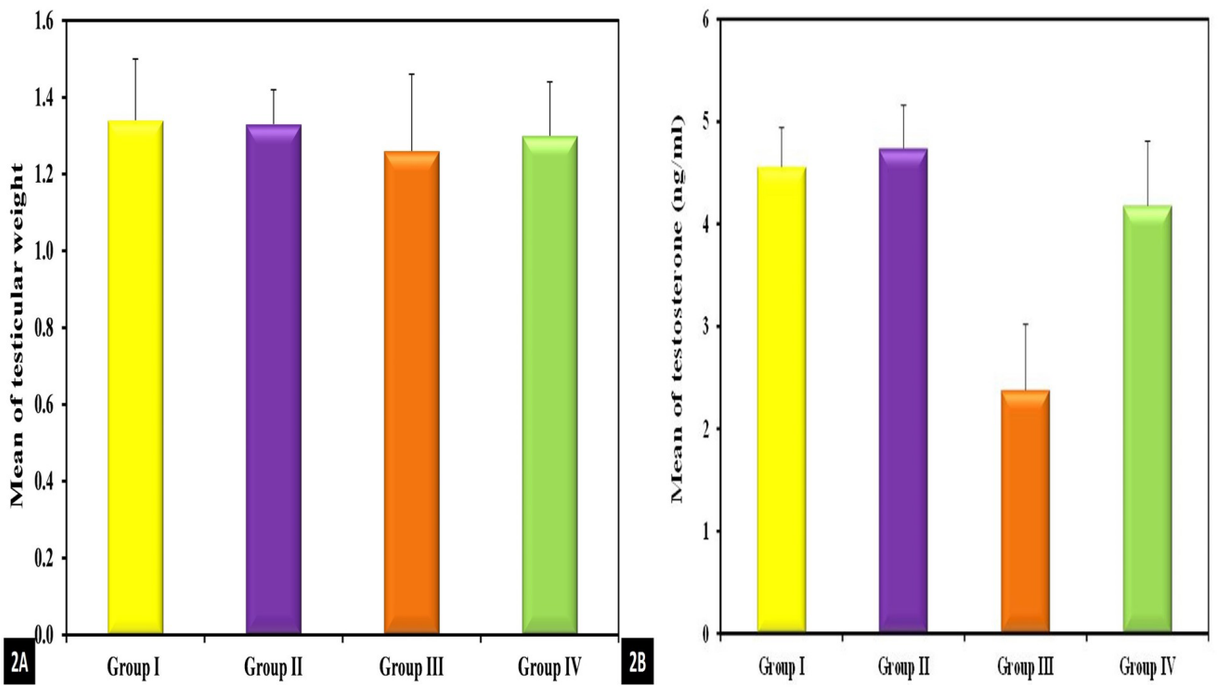

Fig. 2A-B: Bar charts showing comparison between the studied groups according to: A) Testicular weight in grams and B) serum testosterone level (ng/ml).

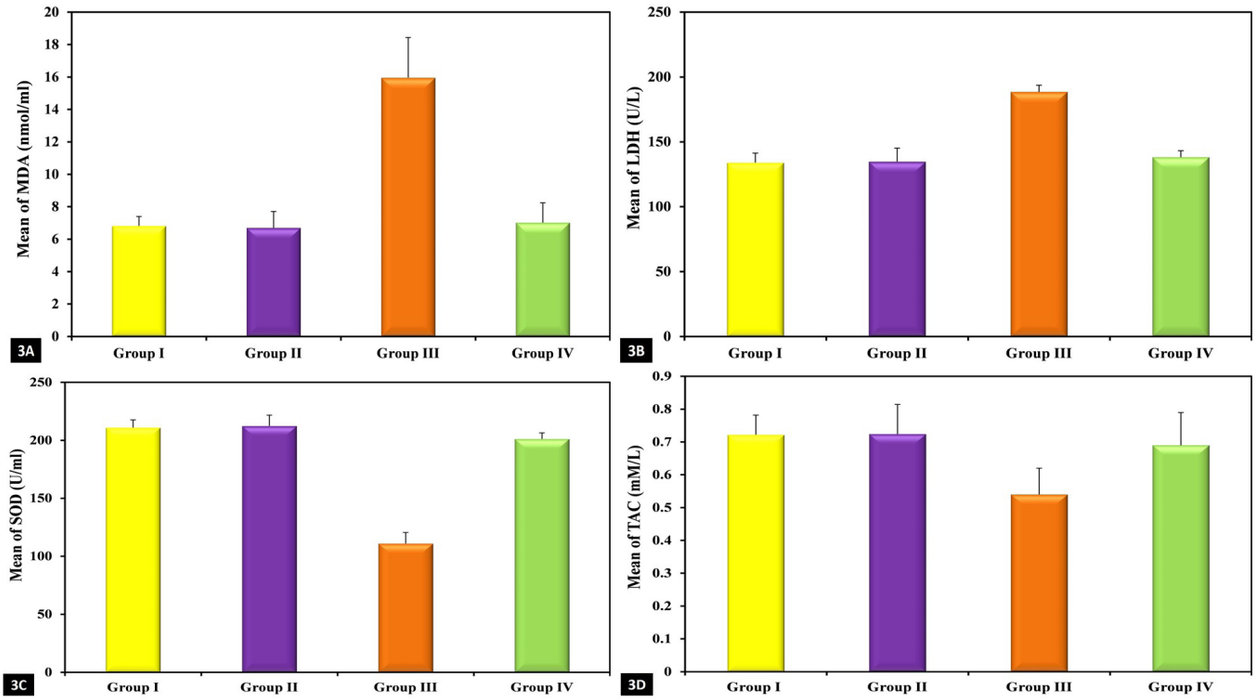

Fig. 3A-D: Bar charts showing comparison between the studied groups according to the mean serum levels of: A) MDA (nmol/ml), B) LDH (U/L), C) SOD (U/ml) and D) TAC (mM/L).

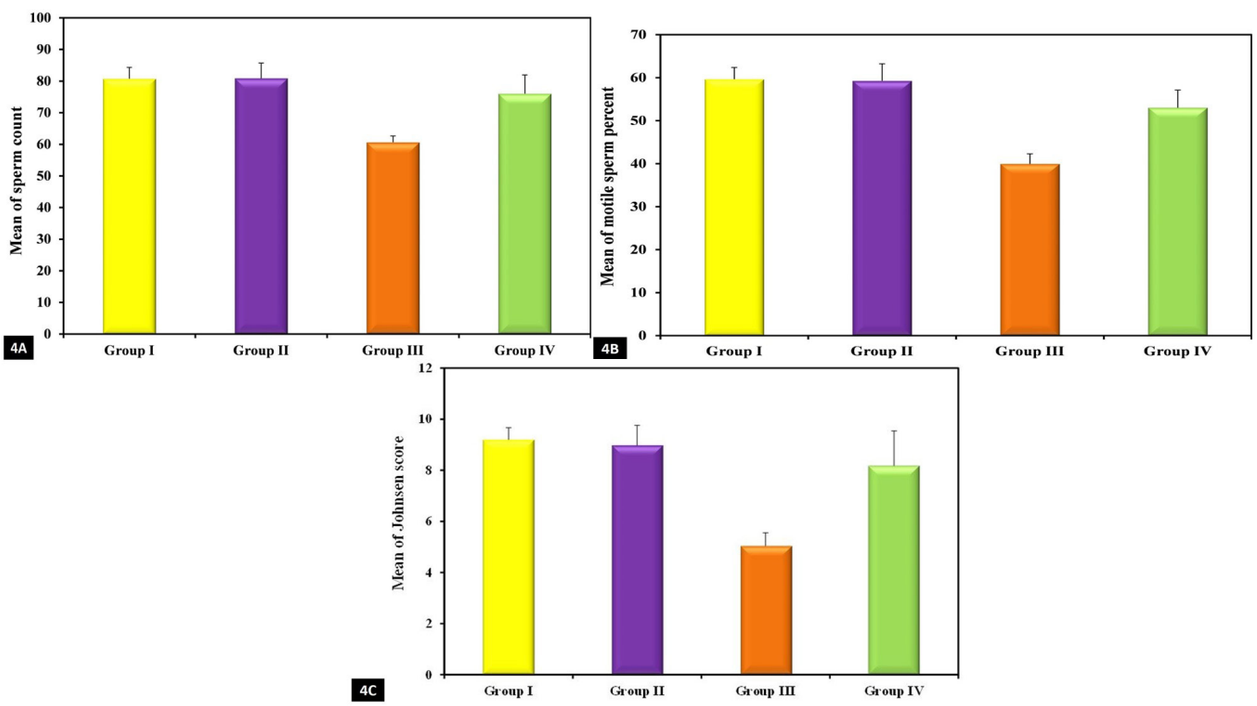

Fig. 4A-C: Bar charts showing comparison between the studied groups according to: A) Sperm count, B) sperm motile percent and C) Johnsen score.

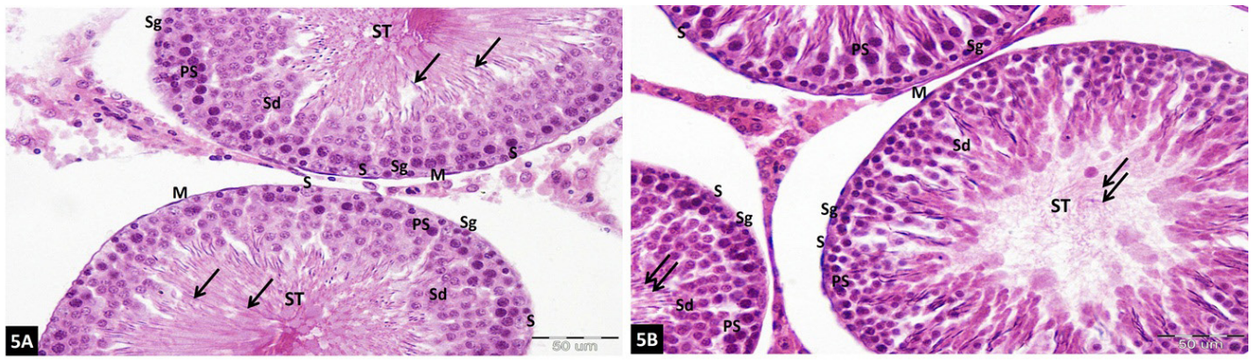

Fig. 5A-B: Photomicrographs of rat testis; A) Control group (group I), B) GSPE group (group II) showing parts of adjacent seminiferous tubules (ST) separated by a narrow interstitium. Each tubule is lined by Sertoli cells (S), spermatogonia (Sg),primary spermatocytes (PS) and early spermatids (Sd).Multiple spermatozoa (↑) are seen filling the lumen of ST. Peritubular myoid cells (M) are also noticed. Mic. Mag. X400.

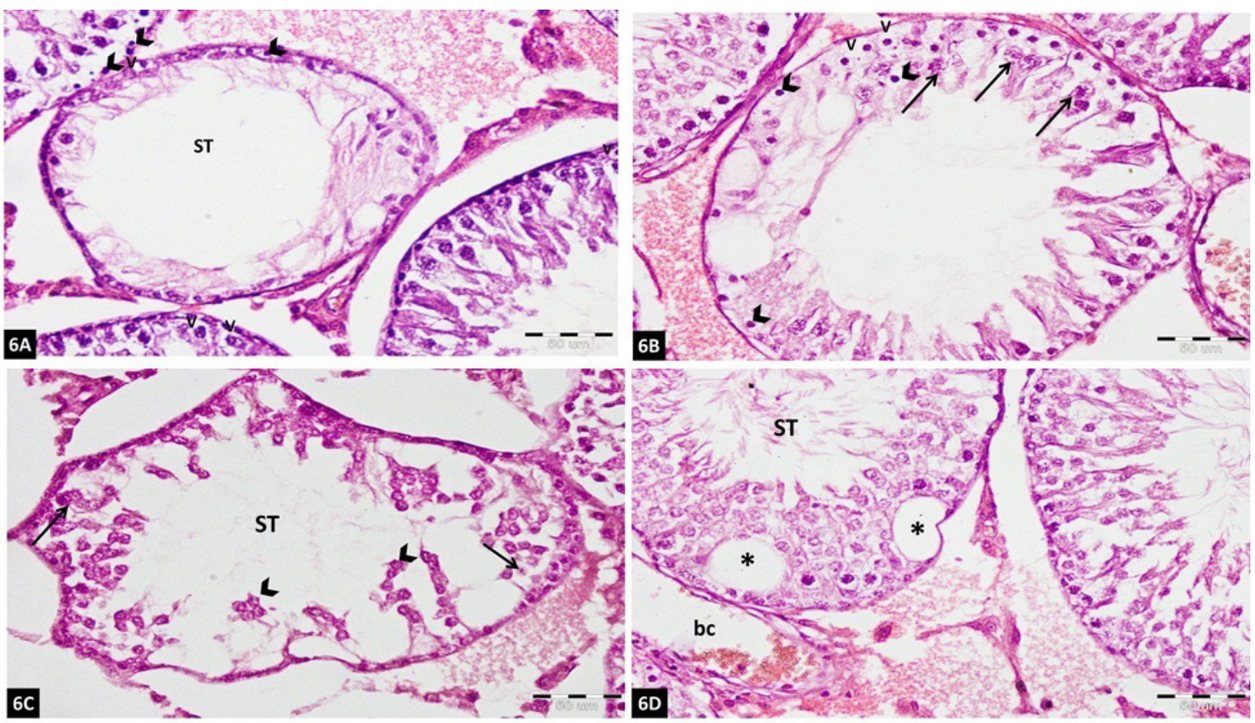

Fig. 6A-D: Photomicrographs of rat testis (group III) which received AL2O3-NPs showing evident histological changes: A) reduction in the number of the lining cells of the ST, some of these cells are vacuolated (V) while others depict dark nuclei (^). B) Degenerating spermatogenic cells (↑), cells with vacuolations (V) and others with small and dark nuclei (^). C) Distortion of the normal architecture of the ST with irregular outline, degenerating spermatogenic cells (↑) and exfoliated cells (^). D) Muliple vacuolations (*) in the ST together with congestion of the blood capillaries (bc). Mic. Mag. x400.

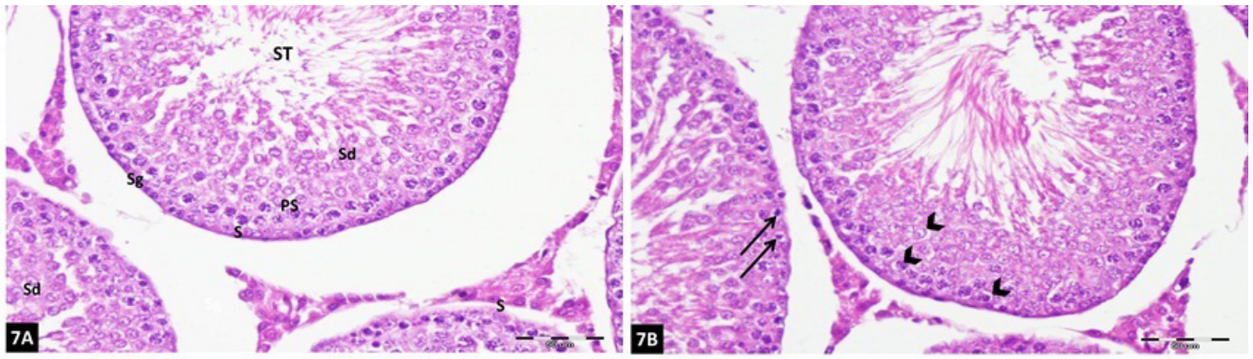

Fig. 7A-B: Photomicrographs of rat ST (group IV) that received AL2O3-NPs and GSPE showing: A) Apparently normal ST with normal lining cells; Sertoli cell (S), spermatogonium (Sg), primary spermatocytes (PS) and early spermatids (Sd). B) Few spermatogenic cells depict vacuolations (^), while others exhibit pyknotic nuclei (↑). Mic. Mag. x400.

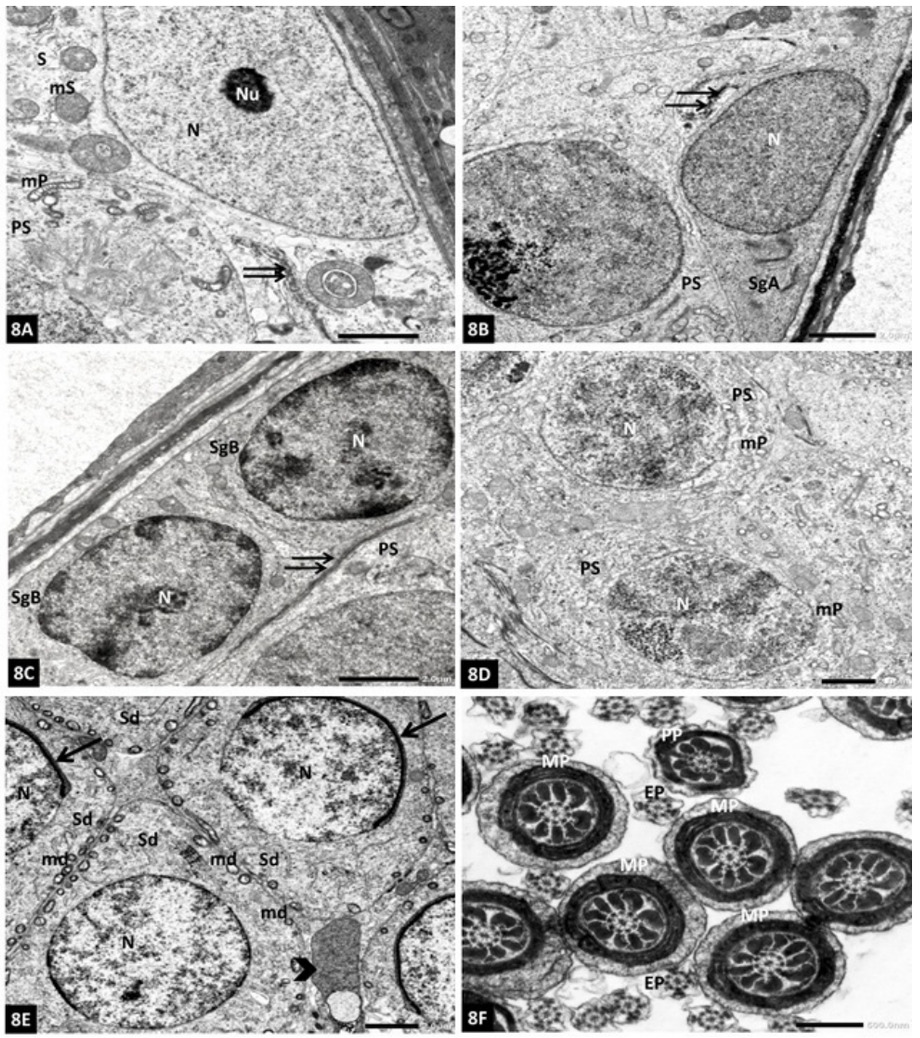

Fig. 8A-F: Electron micrographs of control rat testis (group I) revealing: A) Sertoli cell (S) with a large euchromatic nucleus (N) and a prominent nucleolus (Nu), mS; mitochondria of Sertoli cell, PS; part of a primary spermatocyte above an intact blood testis barrier (↑↑),mP: mitochondria of primary spermatocytes. B) Type A spermatogonium (SgA) shows an ovoid euchromatic nucleus (N) with finely granular chromatin, (↑↑); a blood testis barrier, (PS); a part of a primary spermatocyte. C) Two adjacent type B spermatogonia (SgB) with rounded nuclei (N) and condensed chromatin along the nuclear envelope, (↑↑) an intact blood testis barrier, (PS); a part of a primary spermatocyte. D) Two primary spermatocytes (PS) with large rounded nuclei (N) and multiple mitochondria (mP). E) Four adjacent early spermatids (Sd) depict euchromatic nuclei (N) and multiple peripheral mitochondria (md), an acrosomal cap (↑) is noticed, (^) a residual body. F) Multiple cut sections through sperm tails: middle piece (MP), principal piece (PP) and end piece (EP). Mic. Mag. A&C) x3000, B&D) x2500, E) x2000, F) x10.000.

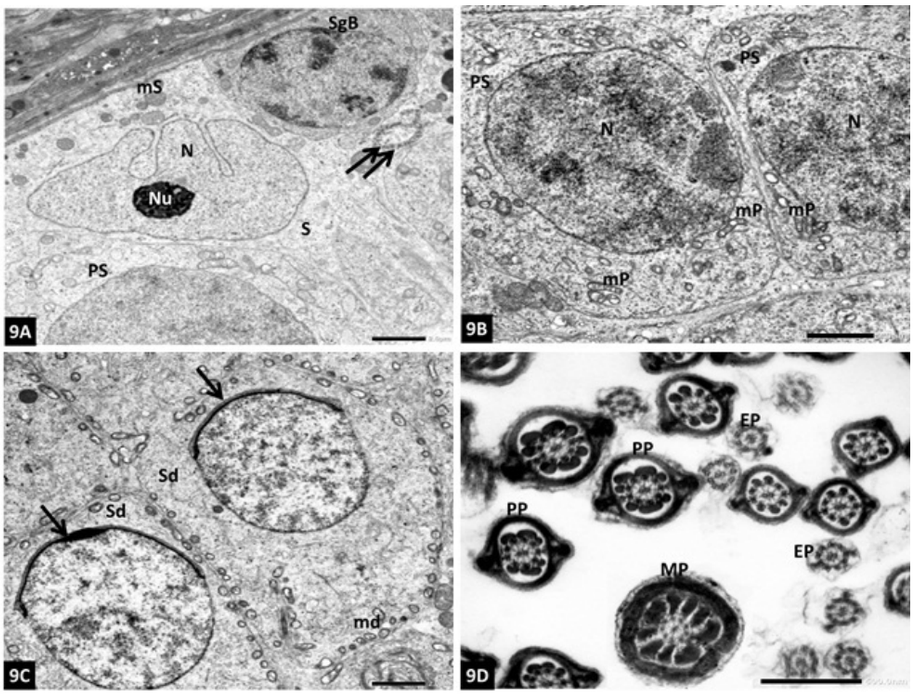

Fig. 9A-D: Electron micrographs of rat seminiferous tubules (group II) that received GSPE showing normal Sertoli cell and spermatogenic cells: A) Sertoli cell (S) with a large irregular nucleus (N), a prominent nucleolus (Nu) and mitochondria (mS), type B spermatogonium (SgB) below a blood testis barrier (↑↑) and part of a primary spermatocyte (PS) are observed. B) Two adjacent primary spermatocytes (PS) with rounded nuclei (N) and mitochondria (mP). C) Two adjacent early spermatids (Sd) with acrosomal caps (↑), md; mitochondria. D) Sections through the sperm tails: principal pieces (PP), end pieces (EP) and middle pieces (MP). Mic. Mag. A&C) x2000, B) x2500, D) x10.000.

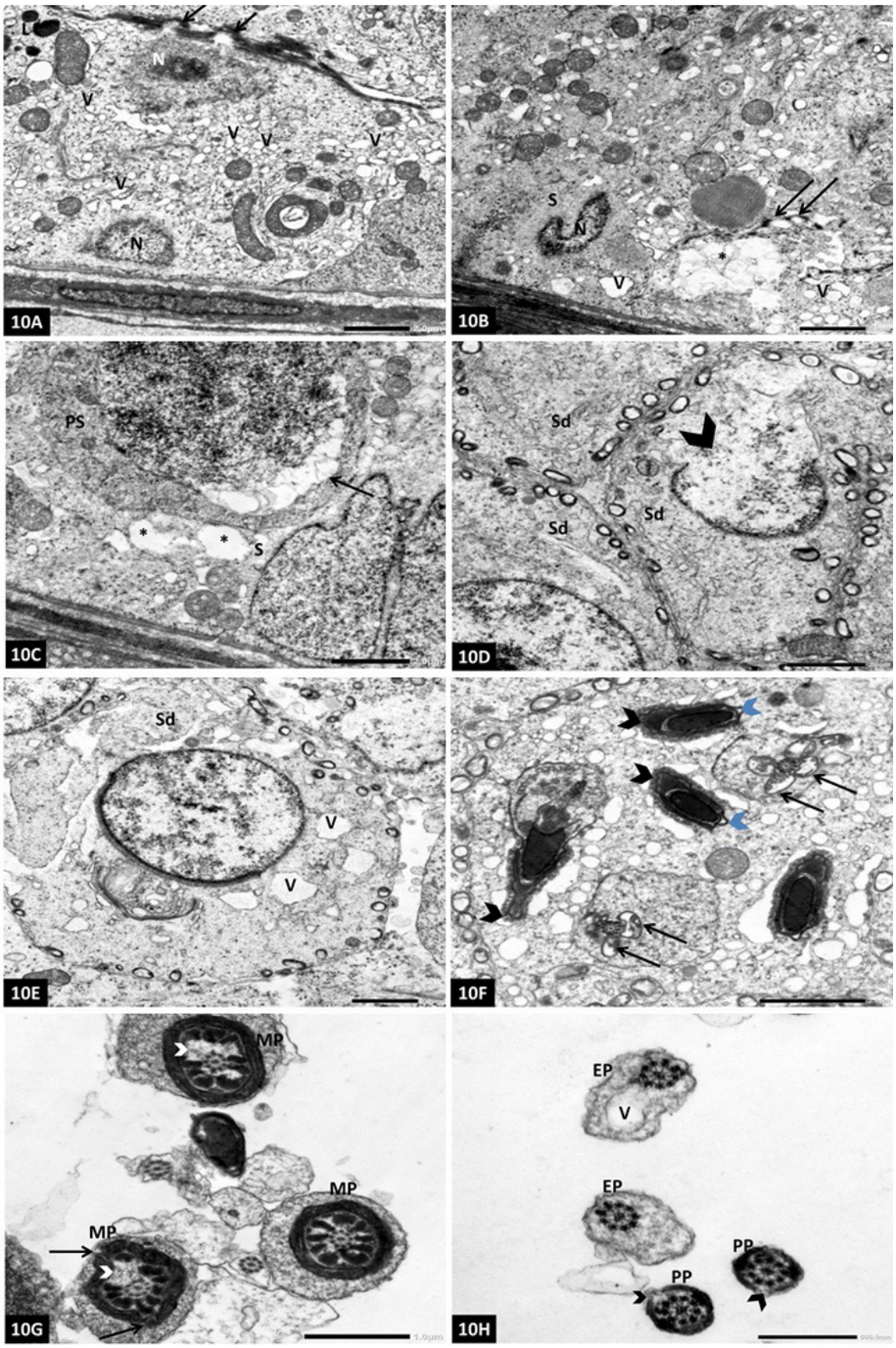

Fig. 10A-H: Electron micrographs of rat testis (group III) received AL2O3-NPs showing evident ultrastructural changes in Sertoli cells as well as the spermatogenic cells: A) Loss of the normal cellular appearance of the ST with numerous vacuoles (V), degenerating nuclei (N) together with disrupted blood testis barrier (↑) and multiple lysosomes (L). B) Sertoli cell (S) with shrunken nucleus (N) and disintegrated chromatin, multiple vacuolations (V), area of rarified cytoplasm (*) and disrupted blood testis barrier (↑↑) are noticed. C) A primary spermatocyte (PS) depicts dilated and vacuolated perinuclear cisterna (↑), rarified cytoplasm (*) of Sertoli cell (S). D) An early spermatid (Sd) showing ruptured nuclear envelope (^). E) Multiple vacuolations (V) are depicted in the cytoplasm of another early spermatid (Sd). F) Abnormal heads of late spermatids (blue ^) with irregular distorted acrosomes (black ^) and vacuolated disrupted mitochondrial sheath (↑). G) Middle pieces (MP) of the sperm tail with distorted outer dense fibers (^) and irregularly arranged mitochondrial sheath (↑). H) Principal pieces (PP) with disrupted circumferential ribs (^), an end piece (EP) with vacuolation (V). Mic. Mag. A,B&E) x2500, C&D) x3000, F) x4000, G) x8000, H) x15.000.

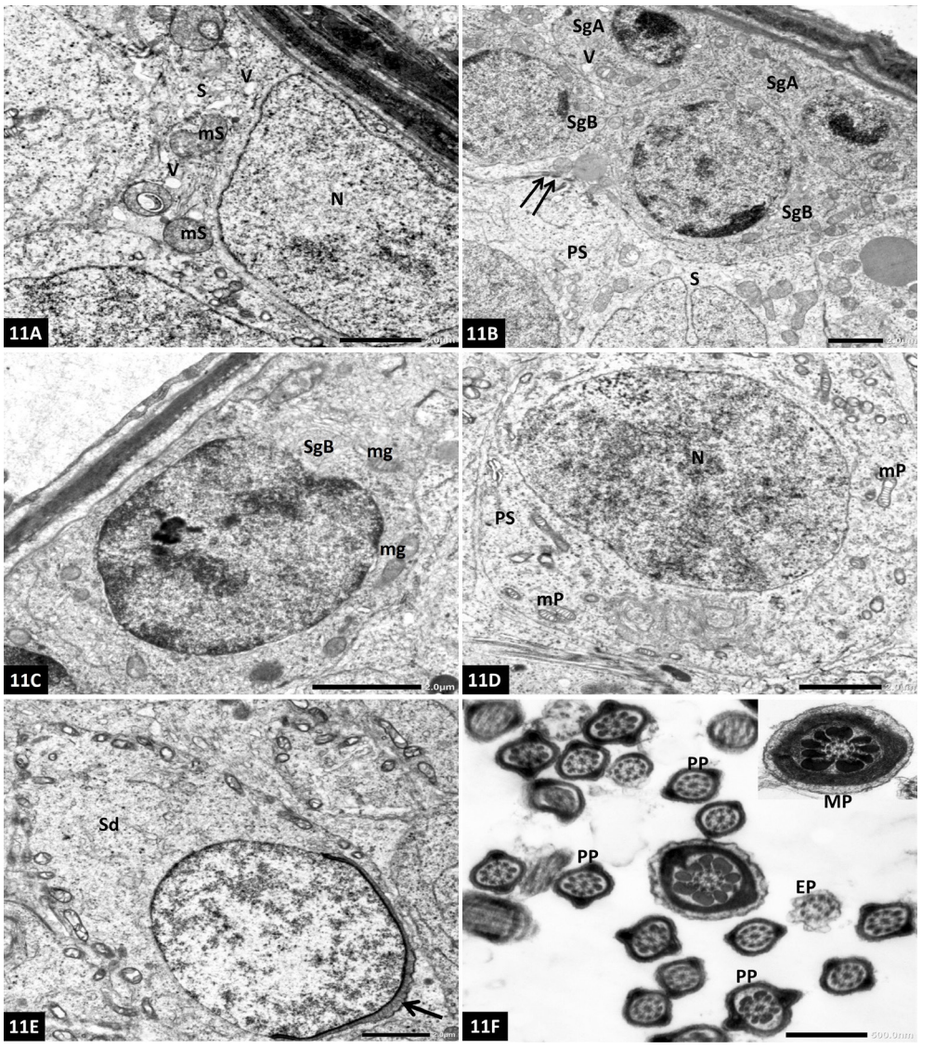

Fig. 11A-F: Electron micrographs of rat ST (group IV) that received AL2O3-NPs and GSPE depict apparently normal Sertoli cells and spermatogenic cells: A) Sertoli cell (S) with a large euchromatic nucleus (N) and multiple mitochondria (mS), some vacuolations (V) are still depicted. B)Two adjacent type A spermatogonia (SgA) lying directly on the basal lamina, two type B spermatogonia (SgB), a part of Sertoli cell (S) and a part of primary spermatocyte (PS), an intact blood testis barrier (↑) appears, mild cytoplasmic vacuolations (V) are encountered. C) Type B spermatogonium (SgB), mg; mitochondria of spermatogonia. D) A primary spermatocyte (PS) with a rounded nucleus (N) and mitochondria (mP). E) An early spermatid (Sd) with an acrosomal cap (↑). F) Multiple cut sections of sperm tails; principal pieces (PP), end pieces (EP), middle piece (MP) inside the inset. Mic. Mag. A&D) x3000, B) x2000, C) x4000, E) x2500, F) x12.000, inset x15000.

DISCUSSION

Throughout the last years, nanoparticles (NPs) have gained wide interest all over the world owing to their diverse applications in all industrial fields including biomedicine[51]. Metal oxide nanoparticles (MONPs) are booming along the last decades due to their small sizes which facilitate their permeation into the versatile body cells[52]. Despite the enormous advantages of these small sized particles, many toxic potential effects on human health have been raised[53]. NPs disseminate through the blood circulation and accumulate in many organs including liver, kidney, brain and reproductive system[54]. Generation of reactive oxygen species (ROS) is considered the main factor underlying the NPs toxic effect[55,56]. It is well established that the dose, the duration, the size and other physio-chemicalnproperties of the NPs are the cornerstones in determining the degree of the particles' toxicity on the cellular level[57]. Among these MONPs, AL2O3-NPs exposure has gained more concern due to their diverse applications[58,59]. It was found that AL2O3- NPs might possibly enter ecosystem during their production, use or even disposal and hence impact the human health[59]. Even though, some studies reported that Al2O3- NPs have a lesser toxicity than the other MONPs[60-64], other studies revealed that the toxicity of AL2O3-NPs is greater than the nanoparticles of the same size[22,65-67].

MONPs have the capacity to cross the BTB that protects the spermatogenic cells, and accumulate within the cells. Consequently, spermatogenesis is affected and the sperm parameters are altered[68]. They also exert negative effects on the interstitial Leydig cells through interfering with the process of steroidogenesis with

decline in the level of serum testosterone hormone[40]. This could explain the recorded decrease in the testosterone level in group III in the present study. Furthermore, the current study showed that administration of AL2O3-NPs led to marked structural changes in the rat seminiferous tubules with distortion of the normal architecture as well as degenerative changes affecting both the spermatogenic and Sertoli cells. Vacuolar formation, rarified cytoplasm and nuclear changes were all encountered. The BTB was seen disrupted in this study which reflects the loss of the Sertoli cell cytoskeleton mainly actin filaments by NPs intoxication. Moreover, MONPs cause down-regulation of the tight junction proteins resulting in impairment of this protective barrier[69,70]. These findings were in accordance to the results of other researchers who reported distortion of the seminiferous tubules with detachment as well as sloughing of the spermatogenic cells within the lumen in the rats treated with AL2O3-NPs. Additionally, they found many spermatogenic cells as well as interstitial Leydig cells with pyknotic nuclei[40].

AL2O3-NPs exert their toxic effect mainly through disturbance of the normal balance between the oxidants and antioxidants levels[71]. Normally, ROS generation as a result of NPs toxicity is overcome by production of antioxidants which act as scavengers to protect the cells[51]. Despite this natural protective response by the body, overproduction of these oxidants cannot be overwhelmed, with resultant toxicity of the cells, tissues and organs[72]. Oxidative stress leads to lipid peroxidation, DNA degradation and inflammation[73]. They also alter the expression of genes that control the mitochondrial functions[72]. Persistent stress exerted on the cell, leads to activation of the cellular adaptive responses with production of the cytochrome C from the malfunctioned mitochondria resulting in cell apoptosis[56]. In the current work, a significant elevation of oxidant markers (MDA and LDH) in concomitant with a dramatic reduction in the antioxidants (TAC and SOD) were detected in the sera of the rats administrated AL2O3-NPs. These changes are suggested to be the leading cause of the cytoplasmic and nuclear changes observed in the current study together with a decrease in the sperm parameters, Johnsen score and serum testosterone.

In accordance with the results of the present work, other investigators reported similar degenerative changes occurring in the seminiferous tubules following administration of AL2O3-NPs together with marked reduction in the antioxidant markers and elevation in the oxidative stress markers[74]. AL2O3-NPs are well known to have a remarkable genotoxic effect mainly through induction of ROS which result in DNA damage and eventually cell death[14]. The reduction in the antioxidant power of the cells in AL2O3-NPs toxicity was attributed to the production of excess superoxide radicles with subsequent elevation in hydrogen peroxide level. Additionally, ROS generation decreases the activities of the antioxidant enzymes and increases the activities of the oxidant one in a dose-dependent manner[36].

Reduction in the percent of the motile sperm was reported in the current work. It could be explained by generation of oxidative stress as well as lipid peroxidation[75,76]. It is well known that the sperm plasma membrane is more susceptible to the oxidant effects owing to its high content of unsaturated fatty acids together with low antioxidant protective capacity. Subsequently, disruption of the lipid components of the plasma membrane will affect its integrity and eventually loss of the sperm motility and occurrence of abnormal sperm[75].

The main grape seed extract (GSE); proanthocyanidin is a natural plant polyphenols, which is a powerful antioxidant and a free radical scavenger. Its effect is more pronounced than vitamins E and C which are considered as potent antioxidants and even superb radical scavenger than carotenoids like beta carotene[77].

In the present work, concomitant administration of GSE with AL2O3-NPs resulted in preservation of the histological architecture of the seminiferous tubules with a statistically significant higher sperm parameters, antioxidant enzymes together with a statistically significant lower MDA and LDH in the sera. The use of GSE in testicular torsion was reported to prevent the elevation of MDA, apoptosis and testicular damage together with improving of Johnsen score[78]. Additionally, GSE with its powerful antioxidant effect, alleviated the toxic effect of cadmium induced testicular damage via attenuating the oxidative stress, reducing apoptosis as well as inflammation[38].

Nuclear factor E2-related factor 2 (Nrf2) is a transcription factor that up-regulates the expression of the antioxidant proteins with a subsequent elevation in their cellular level. On studying the effect of GSE on varicocele, the researchers stated that Nrf2 and its downstream gene HO-1 increased in cases of varicocele due to oxidative stimulation triggered by damage of the testis. Meanwhile, administration of GSE activated Nrf2 pathway via a significant up-regulation of Nrf2 and HO-1with resultant attenuation of the oxidative markers and increase in antioxidant enzymes. However, in their study, the activation of Nrf2 was reported in all groups that received GSE even in the absence of varicocele which means that GSE activates this pathway in the normal and diseased testes[79].

A statistically significant elevation in the testosterone level was noticed in the current work after co-administration of GSE and AL2O3-NPs in group IV. This elevation was interpreted by a group of researchers who studied the role of GSE on cisplatin-induced testicular toxicity. They found that GSE can revert the inhibitory effect of cisplatin on interstitial Leydig cells via up-regulation of mRNA expression of the testosterone synthetase, thus rescued the down-regulation of testosterone synthesis by increasing the expression of the essential enzymes responsible for synthesis of the hormone[80].

CONCLUSION

AL2O3-NPs administration produced a harmful effect on the histological structure and the biochemical tests of the seminiferous tubules, emphasizing their role in male infertility. GSPE exerted a protective effect on the testicular tissue regarding their structure, sperm parameters, antioxidant markers and testosterone levels concluding that GSPE could ameliorate the AL2O3-NPs induced testicular changes. Thus, it is recommended to raise the public awareness of its importance.

CONFLICT OF INTERESTS

There are no conflicts of interest.

REFERENCE

1. Abdelazeim SA, Shehata NI, Aly HF, Shams SGE. Amelioration of oxidative stress-mediated apoptosis in copper oxide nanoparticles-induced liver injury in rats by potent antioxidants. Sci Rep 2020; 10(1):10812.
2. Luo Y, Wang Q, Zhang Y. Biopolymer-based nanotechnology approaches to deliver bioactive compounds for food applications: a perspective on the past, present, and future. J Agric Food Chem 2020; 68(46):12993-13000.
3. Aleixandre-Tudó JL, Bolaños-Pizarro M, Aleixandre JL, Aleixandre-Benavent R. Worldwide scientific research on nanotechnology: a bibliometric analysis of tendencies, funding, and challenges. J Agric Food Chem 2020; 68(34):9158-70.
4. Ojemaye MO, Adefisoye MA, Okoh AI. Nanotechnology as a viable alternative for the removal of antimicrobial resistance determinants from discharged municipal effluents and associated watersheds: A review. J Environ Manage 2020; 275:111234.
5. Medina-Cruz D, Mostafavi E, Vernet-Crua A, Cheng J, Shah V, Cholula-Diaz JL, *et al*. Green nanotechnology-based drug delivery systems for osteogenic disorders. Expert Opin Drug Deliv 2020; 17(3):341-56.
6. Zhou J, Kroll AV, Holay M, Fang RH, Zhang L. Biomimetic nanotechnology toward personalized vaccines. Adv Mater 2020; 32(13):e1901255.
7. Wang W, Mattoussi H. Engineering the bio-nano interface using a multifunctional coordinating polymer coating. Acc Chem Res 2020; 53(6):1124-38.
8. Lawson TB, Mäkelä JTA, Klein T, Snyder BD, Grinstaff MW. Nanotechnology and osteoarthritis; part 1: Clinical landscape and opportunities for advanced diagnostics. J Orthop Res 2021; 39(3):465-72.
9. Xie Z , Fan T , An J , Choi W , Duo Y , Ge Y , *et al*. Emerging combination strategies with phototherapy in cancer nanomedicine. Chem Soc Rev 2020; 49(22):8065-87.
10. Chen D, Fang Z, Ma X, Li Z, Lin H, Ying W, *et al*. Rational design of a Fe/S/N/C catalyst from ZIF-8 for efficient oxygen reduction reaction. Nanotechnology 2020; 31(47):475404.
11. Svendsen C, Walker LA, Matzke M, Lahive E, Harrison S, Crossley A, *et al*. Key principles and operational practices for improved nanotechnology environmental exposure assessment. Nat Nanotechnol 2020; 15(9):731-42.
12. Li Z, Wray PR, Su MP, Tu Q, Andaraarachchi HP, Jeong YJ, *et al*. Aluminum oxide nanoparticle films deposited from a nonthermal plasma: Synthesis, characterization, and crystallization. ACS omega 2020; 5(38):24754-61.
13. Waleczek M, Dendooven J, Dyachenko P, Petrov AY, Eich M, Blick RH, *et al*. Influence of alumina addition on the optical properties and the thermal stability of titania thin films and inverse opals produced by atomic layer deposition. Nanomaterials (Basel) 2021; 11(4):1053.
14. Zhang Q, Wang H, Gea C, Duncan J, He K, Adeosun SO, *et al*. Alumina at 50 and 13nm nanoparticle sizes have potential genotoxicity. J Appl Toxicol 2017; 37(9):1053-64.
15. Czerwinski F. Thermal stability of aluminum alloys. Materials (Basel) 2020; 13(15):3441.
16. Zakiyyan N, Darr CM, Chen B, Mathai C, Gangopadhyay K, McFarland J, *et al*. Surface plasmon enhanced fluorescence temperature mapping of aluminum nanoparticle heated by laser. Sensors (Basel) 2021; 21(5):1585.
17. Nikolova MP, Chavali MS. Metal oxide nanoparticles as biomedical materials. Biomimetics (Basel) 2020; 5(2):27.
18. Spoială A, Ilie CI, Ficai D, Ficai A, Andronescu E. Chitosan-based nanocomposite polymeric membranes for water purification-A review. Materials (Basel) 2021; 14(9):2091.
19. Al-Murshedy NAK, Fares BH. Pathological effect of aluminum hydroxide compared with polymer-based nanoparticles on neonatal mice brain. Ann trop med public health 2020; 23(S19): SP232101.
20. Yoshikawa, AH, Possebon, L, Costa SDS, Souza H, Girol A, Pereira MdL. Adverse effects of metal-based nanoparticles on male reproductive cells. Top 10 Contributions on Environmental Healt; Avid Science 2018:1–19.
21. Hamdi H, Hassan MM. Maternal and developmental toxicity induced by nanoalumina administration in albino rats and the potential preventive role of the pumpkin seed oil. Saudi J.Biol. Sci. 2021; 28(8):4778-85.

22. Balasubramanyam A, Sailaja N, Mahboob M, Rahman MF, Hussain SM , Grover P. In *vivo* genotoxicity assessment of aluminium oxide nanomaterials in rat peripheral blood cells using the comet assay and micronucleus test. Mutagenesis 2018;24 (3):245-51.

23. Jørgensen N, Asklund C, Carlsen E, Skakkebæk NE. Coordinated European investigations of semen quality: results from studies of Scandinavian young men is a matter of concern. Int J Androl 2006; 29(1):54-61.

24. Levine H, Jørgensen N, Martino-Andrade A, Mendiola J, Weksler-Derri D, Mindlis I, *et al*. Temporal trends in sperm count: a systematic review and meta-regression analysis. Hum Reprod update 2017; 23(6):646-59.

25. Agarwal A, Mulgund A, Hamada A, Chyatte MR. A unique view on male infertility around the globe. Reprod Biol Endocrinol 2015; 13(1):1-9.

26. Tang Y, Chen B, Hong W, Chen L, Yao L, Zhao Y, *et al*. ZnO nanoparticles induced male reproductive toxicity based on the effects on the endoplasmic reticulum stress signaling pathway. Int J Nanomed 2019; 14:9563.

27. Soltaninejad H, Zare-Zardini H, Hamidieh AA, Sobhan MR,Banadaky SH,Amirkhani MA, *et al*. Evaluating the toxicity and histological effects of Al2O3 nanoparticles on bone tissue in animal model: A case-control study. J Toxicol 2020; 2020:8870530.

28. Man AWC, Li H, Xia N. Impact of lifestyles (Diet and Exercise) on vascular health: Oxidative stress and endothelial function. Oxid Med Cell Longev 2020; 2020:1496462.

29. Gutierrez-Docio A, Almodóvar P, Moreno-Fernandez S, Silvan JM, Martinez-Rodriguez AJ, Alonso GL, *et al*. Evaluation of an integrated ultrafiltration/solid phase extraction process for purification of oligomeric grape seed procyanidins. Membranes 2020; 10(7):147.

30. Liu M, Yun P, Hu Y, Yang J, Khadka RB, Peng X. Effects of grape seed proanthocyanidin extract on obesity. Obesity Facts 2020; 2(2):279-91.

31. Grandhaye J, Douard V, Rodriguez-Mateos A, Xu Y, Cheok A, Riva A, *et al*. Microbiota changes due to grape seed extract diet improved intestinal homeostasis and decreased fatness in parental broiler hens. Microorganisms 2020; 8(8):1141.

32. Sochorova L, Prusova B, Cebova M, Jurikova T, Mlcek J, Adamkova A, *et al*. Health effects of grape seed and skin extracts and their influence on biochemical markers. Molecules 2020; 25(22):5311.

33. Gupta M, Dey S, Marbaniang D, Pal P, Ray S, Mazumder B. Grape seed extract: Having a potential health benefits. J Food Sci Technol 2020; 57(4):1205-15.

34. West BJ, Deng S, Palu AK. Vitamin C, grape seed extract and citrus bioflavonoids protect the skin against photoaging: a review. JBSM 2020; 8(12):116-34.

35. Nallathambi R, Poulev A, Zuk JB, Raskin I. Proanthocyanidin-rich grape seed extract reduces inflammation and oxidative stress and restores tight junction barrier function in Caco-2 colon cells. Nutrients 2020; 12(6):1623.

36. Srikanth K, Mahajan A, Pereira E, Duarte AC, Venkateswara Rao J. Aluminium oxide nanoparticles induced morphological changes, cytotoxicity and oxidative stress in Chinook salmon (CHSE-214) cells. J Appl Toxicol 2015; 35(10):1133-40.

37. Park SH, Lim JO, Kim WI, Park SW, Lee SJ, Shin IS, *et al*. Subchronic toxicity evaluation of aluminum oxide nanoparticles in rats following 28-day repeated oral administration. BiolTrace Elem Res 2021; 18:12011-21.

38. Sönmez MF, Tascioglu S. Protective effects of grape seed extract on cadmium-induced testicular damage, apoptosis, and endothelial nitric oxide synthases expression in rats. Toxicol Ind Health 2016; 32(8):1486-94.

39. Morsi AA, Shawky LM, El Bana EA. The potential gonadoprotective effects of grape seed extract against the histopathological alterations elicited in an animal model of cadmium-induced testicular toxicity. Folia Morphologica 2020;79(4):767-76.

40. Yousef MI, Al-hamadani M, Kamel M. Reproductive toxicity of aluminum oxide nanoparticles and zinc oxide nanoparticles in male rats. Nanoparticle 2019; 1(1):3.

41. Aledani AH, Khudhair NA, Alrafas HR. Effect of different methods of anesthesia on physiobiochemical parameters in laboratory male rats. Basra J Vet Res 2020;19:206-14.

42. Gazia MA. Histological study on the possible ameliorating effect of platelet rich plasma on ischemia/ reperfusion injury in testicular torsion model in adult albino rat. Egypt J Histol 2020; 43(2):614-29.

43. Draper HH, Hadley M. Malondialdehyde determination as index of lipid Peroxidation. Meth Enzymol 1990; 186:421-31.

44. Jovanovic P, Zoric L, Stefanovic I, Dzunic B, Djordjevic- Jocic J, Radenkovic M, *et al*. Lactate dehydrogenase and oxidative stress activity in primary open-angle glaucoma aqueous humour. Bosn J Basic Med Sci. 2010; 10(1):83-8.

45. Aziz J, Aidaros AE, Ali AF, Sabry MA. Ameliorating effect of alpha-lipoic acid on methotrexate-induced histological and biochemical changes in the lung of adult albino rat. Egypt J Histol 2020; 43(3):878-90.

46. Koracevic D, Koracevic G, Djordjevic V, Andrejevic S, Cosic V. Method for the measurement of antioxidant activity in human fluids. J Clinl Pathol 2001; 54(5):356-61.

47. Vega SG, Guzman P, Garcia L, Espinosa J, Cortinas de Nava C. Sperm shape abnormality and urine mutagenicity in mice treated with niclosamide. Mutat Res. 1988; 204(2):269-76.

48. Bancroft J and Layton C. The hematoxylin and eosin, connective and mesenchymal tissues with their stains. In: Suvarna S, Layton C and Bancroft J (eds). Bancroft's Theory and Practice of Histological Techniques. 7th ed. Churchill Livingstone. Philadelphia. (2013) pp: 173-212.

49. Lewis-Jones DI, Kerrigan DD. A modified Johnsen's count for evaluation of spermatogenesis in the rat. IRCS Med Sci. 1985; 13:510- 11.

50. Kuo J. Electron microscopy: methods and protocols. 2nd ed. Totowa, New Jersy: Humana Press Inc.; 2007. p. 19. ISSN 1064-3745.

51. Khan, I, Saeed, K, Khan I. Nanoparticles: Properties, applications and toxicities. Arab. J. Chem. 2019; 12: 908-31.

52. Sengupta J, Ghosh S, Datta P, Gomes A, Gomes A. Physiologically important metal nanoparticles and their toxicity. J Nanosci Nanotechnol 2014; 14(1):990-1006.

53. Dağlıoğlu Y, Yılmaz Öztürk B. Effect of concentration and exposure time of ZnO-TiO2 nanocomposite on photosynthetic pigment contents, ROS production ability, and bioaccumulation of freshwater algae (Desmodesmus multivariabilis). Caryologia 2018 ;71(1):13-23.

54. Morsy GM, El-Ala KS, Ali AA. Studies on fate and toxicity of nanoalumina in male albino rats: lethality, bioaccumulation and genotoxicity. Toxicol Ind Health 2016; 32(2), 344–59.

55. Santonastaso M, Mottola F, Colacurci N, Iovine C, Pacifico S, Cammarota M, *et al*. In *vitro* genotoxic effects of titanium dioxide nanoparticles (n-TiO2) in human sperm cells. Mol Reprod Dev 2019; 86(10):1369-77.

56. Bara N, Kaul G. Enhanced steroidogenic and altered antioxidant response by ZnO nanoparticles in mouse testis Leydig cells. Toxicol Ind Health 2018; 34(8):571-88.

57. Zhou Q, Yue Z, Li Q, Zhou R, Liu L. Exposure to PbSe nanoparticles and male reproductive damage in a rat model. Environ Sci Technol. 2019; 53(22):13408-16.

58. Tarlani, A, Isari, M, Khazraei A, Eslami Moghadam M. New sol-gel derived aluminum oxide-ibuprofen nanocomposite as a controlled releasing medication. J Nanomed Res 2017: 2(1), 28–35.

59. Pakrashi S, Dalai S, Sabat D, Singh S, Chandrasekaran N, Mukherjee A. Cytotoxicity of Al2O3 nanoparticles at low exposure levels to a freshwater bacterial isolate. Chem Res Toxicol 2011; 24: 1899-904.

60. Lanone S, Rogerieux F, Geys J, Dupont A, Maillot-Marechal E, Boczkowski J, *et al*. Comparative toxicity of 24 manufactured nanoparticles in human alveolar epithelial and macrophage cell lines. Part. Fibre Toxicol 2009; 6: 14.

61. Kim IS, Baek M, Choi SJ. Comparative cytotoxicity of Al2O3, CeO2, TiO2 and ZnO nanoparticles to human lung cells. J Nanosci Nanotechnol 2012; 10: 3453-58.

62. Radzium E, Dudkiewicz Wilczyńska J, Książek I, Nowak K, Anuszewska EL, Kunicki A, *et al*. Assessment of the cytotoxicity of aluminum oxide nanoparticles on selected mammalian cells. Toxicol In *Vitro* 2011; 25: 1694-700.

63. Sun J, Wang S, Zhao D, Hun FH, Weng L, Liu H. Cytotoxicity, permeability, and inflammation of metal oxide nanoparticles in human cardiac microvascular endothelial cells: cytotoxicity, permeability, and inflammation of metal oxide nanoparticles. Cell Biol Toxicol 2011; 27: 333-42.

64. Demir E, Burgucu D, Turna F, Aksakal S, Kaya B. Determination of TiO2, ZrO2, and Al2O3 nanoparticles on genotoxic responses in human peripheral blood lymphocytes and cultured embryonic kidney cells. J Toxicol Environ Health A 2013; 76: 990–1002.

65. Serra A, Letunic I, Fortino V, Handy RD, Fadeel B, Tagliaferri R, *et al*. INSIdE NANO: a systems biology framework to contextualize the mechanism-of-action of engineered nanomaterials. Scientific reports 2019; 9(1):1-0.

66. Sadiq IM, Pakrashi S, Chandrasekaran N, Mukherjee A. Studies on toxicity of aluminum oxide (Al2O3) nanoparticles to microalgae species: Scenedesmus sp. and Chlorella sp. J Nanoparticle Res 2011; 13(8):3287-99.

67. Oesterling E, Chopra N, Gavalas V, Arzuaga X, Lim EJ, Sultana R, *et al*. Alumina nanoparticles induce expression of endothelial cell adhesion molecules. Toxicology letters 2008; 178(3):160-6.

68. Vassal M, Rebelo S, Pereira MD. Metal oxide nanoparticles: evidence of adverse effects on the male reproductive system. Int J Molr Sci 2021; 22(15):8061.

69. Mao Z, Yao M, Xu B, Ji X, Jiang H, Han X, *et al*. Cytoskeletons of two reproductive germ cell lines response differently to titanium dioxide nanoparticles mediating vary reproductive toxicity. J Biomed Nanotechnol 2017; 13(4):409-16.

70. Liu Q, Xu C, Ji G, Liu H, Mo Y, Tollerud DJ, *et al*. Sublethal effects of zinc oxide nanoparticles on male reproductive cells. Toxicol in *Vitro* 2016; 35:131-8.

71. Zhang QL, Li MQ, Ji JW, Gao FP, Bai R, Chen CY, *et al*. In *vivo* toxicity of nano-alumina on mice neurobehavioral profiles and the potential mechanisms. Int J Immunopathol Pharmacol 2011; 24(1):23S-29S.

72. Yousef MI, Mutar TF, Kamel MA. Hepato-renal toxicity of oral sub-chronic exposure to aluminum oxide and/or zinc oxide nanoparticles in rats. Toxicol reports 2019; 6:336-46.

73. Prabhakar PV, Reddy UA, Singh SP, Balasubramanyam A, Rahman MF, Indu Kumari S, *et al*. Oxidative stress induced by aluminum oxide nanomaterials after acute oral treatment in Wistar rats. J ApplToxicol 2012; 32(6):436-45.

74. Hamza RZ, Al-Juaid NS, Althubaiti EH. Antioxidant effect of carnosine on aluminum oxide nanoparticles (Al2O3-NPs)-induced hepatotoxicity and testicular structure alterations in male rats. Int J Pharmacol 2018; 14(5):740-50..

75. Vernet P, Aitken RJ, Drevet JR. Antioxidant strategies in the epididymis. Mol Cell Endocrinol 2004; 216(1-2):31-9.

76. Ogunsuyi OM, Ogunsuyi OI, Akanni O, Alabi OA, Alimba CG, Adaramoye OA, *et al*. Alteration of sperm parameters and reproductive hormones in Swiss mice via oxidative stress after co-exposure to titanium dioxide and zinc oxide nanoparticles. Andrologia 2020; 52(10):e13758.

77. Boghdady NA. Antioxidant and antiapoptotic effects of proanthocyanidin and ginkgo biloba extract against doxorubicin-induced cardiac injury in rats. Cell Biochem Funct 2013; 31(4):344-51.

78. Bayatli F, Akkus D, Kilic E,Saraymen R, Sonmez MF. The protective effects of grape seed extract on MDA, AOPP, apoptosis and eNOS expression in testicular torsion: an experimental study. J Urol 2013; 31(3):615-22.

79. Wang Y, Chen F, Liang M, Chen S, Zhu Y, Zou Z, *et al*. Grape seed proanthocyanidin extract attenuates varicocele induced testicular oxidative injury in rats by activating the Nrf2 antioxidant system. Mol Med Rep 2018; 17(1):1799-806.

80. Tian M, Liu F, Liu H, Zhang Q, Li L, Hou X*et al*. Grape seed procyanidins extract attenuates Cisplatin-induced oxidative stress and testosterone synthase inhibition in rat testes. Syst Biol Reprod Med 2018; 64(4):246-59.

الملخص العربى

الدور التحسينى المحتمل لمستخلص بذور العنب بروانثوسيانيدين على سمية الأنابيب الناقلة للمنى المستحدثة بواسطة جزيئات أكسيد الألومنيوم المتناهية الصغر فى الجرذان البالغة: دراسة نسيجية و كيميائية

ايمان نبيل[١]، مروة محمود ماضى[٢]، سيلفيا كميل صديق ساويرس[١]

[١]قسم الهستولوجيا وبيولوجيا الخلية، [٢]قسم التشريح وعلم الأجنة، كلية الطب، جامعة الاسكندرية

المقدمة: على الرغم من ان جزيئات أكسيد الألومنيوم المتناهية الصغرتستخدم على نطاق واسع ، إلا أن المعلومات عن مخاطرها المحتملة على الجهاز التناسلي الذكري لم تدرس بصورة كاملة. يعد الانتاج الزائد لفصائل الاكسجين هو السبب الرئيسى للتغيرات الهيستولوجية التى تحدثها جزيئات أكسيد الألومنيوم المتناهية الصغرفى العديد من أعضاء الجسم. يعتبرمستخلص بذور العنب بروانثوسيانيدين مركب قوى مضاد للأكسدة ، و يحتمل ان يضعف من هذا التأثير.
الهدف: لتقييم التغيرات الهيستولوجية المستحدثة بواسطة جزيئات أكسيد الألومنيوم المتناهية الصغر على الأنابيب الناقلة للمنى فى الجرذان البالغة وكذلك الدور المحتمل للبروانثوسيانيدين في تخفيف هذه التغييرات.
المواد وطرق البحث: تم تقسيم اربعة وعشرون من ذكور الجرذان البيضاء البالغة إلى اربعة مجموعات متساوية: المجموعة الأولى (المجموعة الضابطة) والمجموعة الثانية تلقت بروانثوسيانيدين بالفم بجرعة ١٠٠ مجم / كجم / يوم و المجموعة الثالثة تلقت ٧٠ مجم / كجم / يوم من جزيئات أكسيد الألومنيوم المتناهية الصغر بالفم, أما المجموعة الرابعة فقد تلقت العلاج المشترك من البروانثوسيانيدين و جزيئات أكسيد الألومنيوم المتناهية الصغر في نفس الجرعات كما في المجموعتان ٢ و ٣.تم التضحية بالجرذان بعد ٢٨ يوم، وتم تجميع عينات الدم لتحليلها كيميائيا. كما تم اخذ عينات من السائل المنوى لعد الحيوانات المنوية و نسبة الحيوانات المنوية المتحركة.وايضاً تم وزن الخصيات ثم تحضيرها و فحصها بالمجهر الضوئي والإلكتروني و حساب مقياس جونسين. تم اجراء التحليل الاحصائى للبيانات التى تم الحصول عليها.
النتائج: نجم عن جزيئات أكسيد الألومنيوم المتناهية الصغر احداث فجوات مع تقليل عدد الخلايا المبطنة للأنابيب الناقلة للمنى. وقد وجدت خلايا مكونة للمنى متنكسة و منفصلة مع رؤوس وذيول غير طبيعية للحيوانات المنوية. بالإضافة إلى ذلك شوهد اضطراب حاجز الخصية الدموي وتغيرات تنكسية لخلايا سيرتولي. كما لوحظ احصائيا انخفاض كبير في مستوى هرمون التستوستيرون في الدم ودلالات مضادات الاكسدة و مقياس جونسين ومعلمات السائل المنوى بالاضافة الى الارتفاع الملحوظ احصائيا لعوامل الأكسدة. نتج عن تعاطى البروانثوسيانيدين مصاحبا لجزيئات أكسيد الألومنيوم المتناهية الصغر تحسنًا في تركيب الخصية مع استعادة المستوى الطبيعي تقريبًا من هرمون التستوستيرون و العوامل المضادة للأكسدة و تحليل السائل المنوى.
الخلاصة: مستخلص بذور العنب البروانثوسيانيدين يضعف التغيرات النسيجية و الكيميائية للخصية الناجمة عن جزيئات أكسيد الألومنيوم المتناهية الصغر . ولذلك فأن الوعى العام باهمية مستخلص بذور العنب البروانثوسيانيدين يعتبر ضروريا.